Structural and biochemical analysis of Ras-effector signaling via RalGDS

I.R. Vetter[a], T. Linnemann[a], S. Wohlgemuth[a], M. Geyer[b], H.R. Kalbitzer[b], C. Herrmann[a], A. Wittinghofer[a,*]

[a] *Max-Planck-Institut für molekulare Physiologie, Abteilung Strukturelle Biologie, Rheinlanddamm 201, D-44139 Dortmund, Germany*
[b] *Institut für Biophysik und Physikalische Biochemie, Universität Regensburg, Universitätsstraße 31, D-93053 Regensburg, Germany*

Received 25 February 1999; received in revised form 8 April 1999

Abstract The structure of the complex of Ras with the Ras-binding domain of its effector RalGDS (RGS-RBD), the first genuine Ras-effector complex, has been solved by X-ray crystallography. As with the Rap-RafRBD complex (Nasser et al., 1995), the interaction is via an inter-protein β-sheet between the switch I region of Ras and the second strand of the RGS-RBD sheet, but the details of the interactions in the interface are remarkably different. Mutational studies were performed to investigate the contribution of selected interface residues to the binding affinity. Gel filtration experiments show that the Ras·RGS-RBD complex is a monomer. The results are compared to a recently determined structure of a similar complex using a Ras mutant (Huang et al., 1998) and are discussed in relation to partial loss-of-function mutations and the specificity of Ras versus Rap binding.

Key words: Ras; Ras-binding domain; Structure; RalGDS; Signaling

1. Introduction

Ras is a major regulator of cell growth and development, and oncogenic mutants of Ras induce transformation of cells. It is a signal switch molecule that cycles between the GDP-bound inactive and the GTP-bound active form. In the active form Ras interacts with effector molecules which are defined as binding tightly to the GTP-bound form. Several effectors have been identified each of which is believed to initiate a cascade of signal transduction reactions, the combination of which is needed for biological activity of Ras [3]. In order to dissect these pathways and define the requirements for each of them, partial loss-of-function mutations have been defined which bind selectively to only a subset of effector molecules [4,5] and have been used to analyze Ras function [6–12].

The major downstream target of Ras is the protein kinase Raf, which activates the MAP kinase (Erk) cascade [13–16]. The structure of the Ras-binding domain (RBD) of c-Raf-1 alone [17] or in complex with a Ras homologue Rap or Raps (=Rap(E30D K31E)), have shown that RafRBD binds to Rap(s) by forming an apparent inter-protein β-sheet involving the effector (switch I) region of Ras [1,18]. Another effector of Ras is RalGDS (for Ral guanine nucleotide dissociation stimulator) [19–21], and its isoforms Rgl, Rlf and Rgl-2 [22–24], all of which have an RBD at the C-terminal end. The structure of the RBD of RalGDS (RGS-RBD from now on) bound to a Ras mutant (E31K) has recently been determined [2]. Here we have solved the structure of Ras itself bound to the RBD of RalGDS and determined the biochemical properties of Ras-RalGDS complexes. The results are discussed in light of the earlier structure [2], the stoichiometry of the complex, partial loss-of-function mutations and signaling properties of Ras and Rap complexes.

2. Materials and methods

2.1. Biochemistry

Mutants of Ras and RGS-RBD, respectively, were generated by standard PCR mutagenesis protocols. The preparation of proteins and the nucleotide exchange procedure is as described [25]. The complex between Ras·GppNHp and RGS-RBD was purified by size exclusion chromatography. For crystallization C-terminally truncated Ras (residues 1–166) was used and full length Ras for biochemical studies. The K_D values for wild-type and mutant proteins were obtained by the GDI method which is based on the observation that the guanine nucleotide dissociation is inhibited (GDI) by RGS-RBD binding as described [25]. For determination of the molecular mass, gel filtration of the Ras·RGS-RBD complex was eluted from a Pharmacia Superdex 75 column (10/30 cm), in 50 mM Tris pH 7.4, 5 mM $MgCl_2$, 2 mM DTE.

2.2. Crystallization and structure determination

The Ras·RGS-RBD complex was crystallized at room temperature from 1.3 M ammonium sulfate, either without additives or with 200 mM MES pH 6.0–6.5 and 100 mM $MgCl_2$. The former solution yielded orthorhombic crystals with space group $C222_1$, $a=53.4$ Å, $b=96.0$ Å, $c=105.9$ Å. The crystals showed a high mosaicity of 2.2°. The latter crystallization solution produced hexagonal $P6_322$ crystals with $a=b=94.3$ Å, $c=164.8$ Å and a mosaicity of 0.6°. The crystals diffracted to 3.4 Å at maximum even at a strong synchrotron beamline. Both crystal forms have one molecule of the complex per asymmetric unit.

Diffraction data were collected on a multi-wire area detector (Nicolet/Xentronics, Madison, WI, USA) using a rotating anode X-ray generator and data sets were processed using the XDS software suite [26]. Both crystal forms were solved by molecular replacement using AMORE [27] and RGS-RBD [28] and Ras-GTP as model. The omitted nucleotide showed up in the difference density indicating the correct solution. However, the density of the missing RGS-RBD moiety did not show up in sufficient quality using one or the other data set by itself. Molecular replacement with the known NMR- and X-ray structures of uncomplexed RGS-RBD [28,29] was unsuccessful. Therefore, multi-crystal averaging was performed in combination with solvent flattening procedures with the program DMMULTI [27]. The resulting electron density map allowed tracing of the missing RGS-RBD backbone (except residues 50–55 and 78–89) and the localization of prominent side chains. Since the maximum resolution of both data sets is only 3.4 Å, the known structures of RGS-RBD had to be used as templates, i.e. stretches of secondary structure elements were moved into the averaged density. Modeling was performed using the program 'O' [30]. All attempts to refine the model failed to improve the free R factor significantly, which is 35.4% for the final model. However, the quality of the averaged density allowed the unambiguous positioning of the RGS-RBD moiety and the analysis of the interactions in the interface. The correctness of the model was indicated by the fact that the modeled RGS-RBD moiety yielded the correct solution in a rotation function search whereas the

*Corresponding author. Fax: +49 (231) 1206230.
E-mail: Alfred.Wittinghofer@mpi-dortmund.mpg.de

PII: S0014-5793(99)00555-4

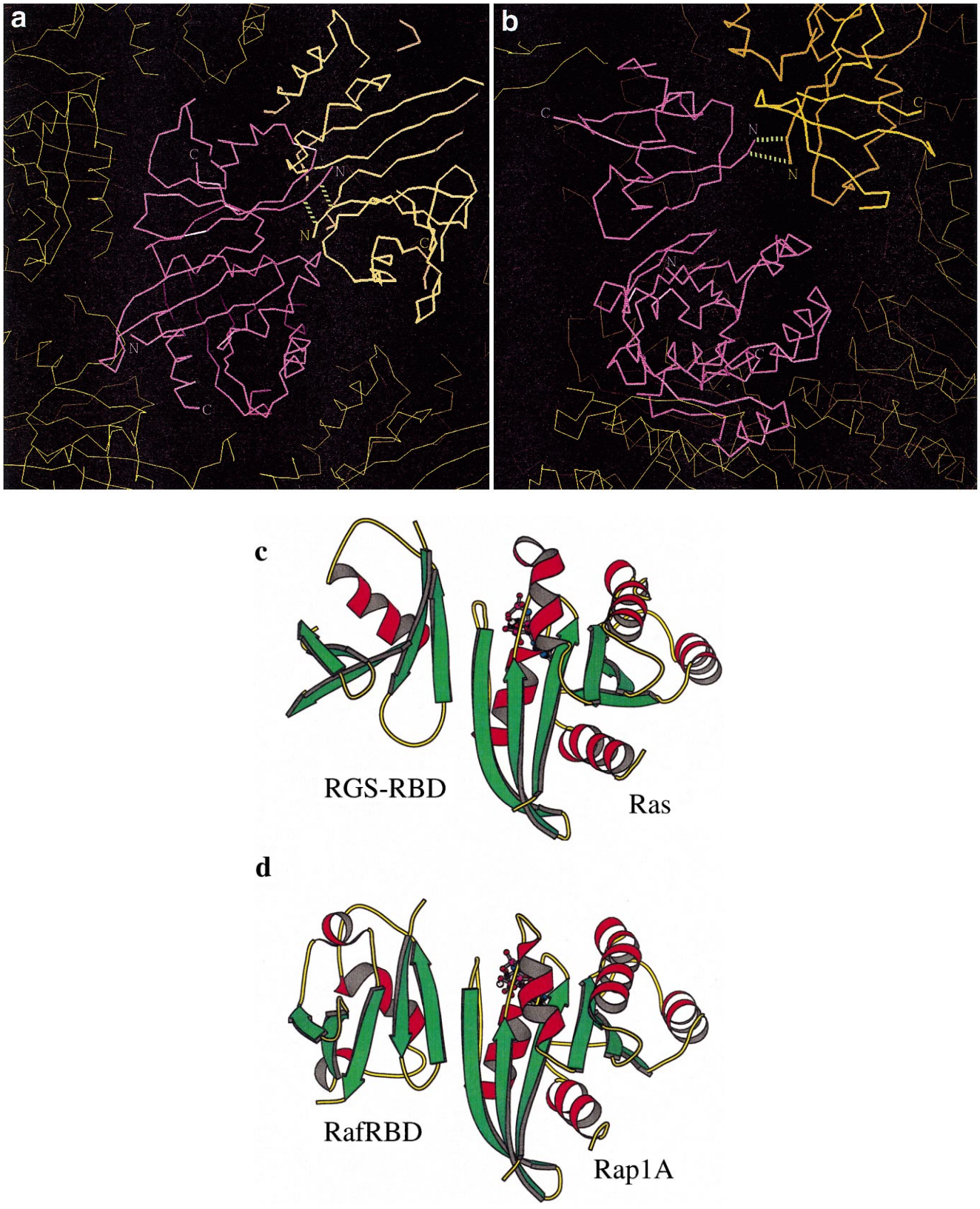

Fig. 1. Structure of the complex. a, b show the different crystal packing of the main chain model in the two space groups with the disulfide bridges between symmetry related molecules highlighted as green, dashed lines (a for space group $C222_1$, b for $P6_322$). c, d show ribbon diagrams of the Ras·RGS-RBD (c) and the Rap·RafRBD (d) complex. The figure was produced with MOLSCRIPT [33].

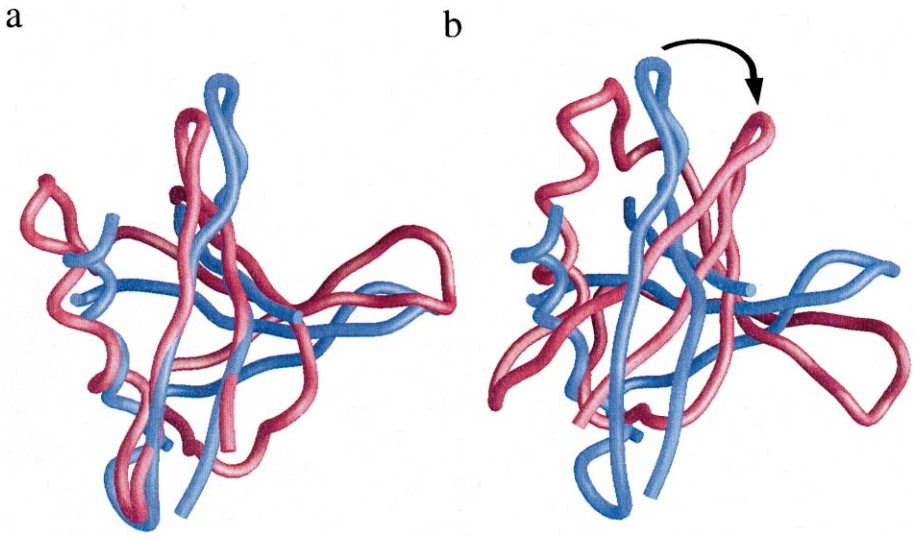

Fig. 2. Overlay of the RafRBD (pink) and RGS-RBD (blue) backbones. In a, the molecules were fitted by a least squares fit procedure using the program 'O' [30]; in b, the Ras and the Rap moieties of the corresponding complexes were fitted on top of each other to show the 'rotation' (arrow) of the RBDs. The figure was drawn using GRASP [34].

NMR- or X-ray model of the RGS-RBD alone did not. The crystallographic data are summarized in Table 1.

3. Results and discussion

3.1. Complex structure

From deletion cloning the Ras-binding domain (RBD) of human RalGDS, RGS-RBD, was defined as a fragment of 97 C-terminal residues (corresponding to residues 790–886, [31]). The structure of RGS-RBD has been solved by heteronuclear NMR spectroscopy as well as X-ray crystallography and was shown to have the same ubiquitin superfold as the Ras-binding domain of the protein kinase c-Raf-1, RafRBD [28,29].

The structure of the Ras·RGS-RBD complex was determined in spite of the relatively poor data quality by multicrystal averaging using two different crystal forms as described in Section 2. No density was visible for residues 50 to 55 and residues 78 to 89 which could be due to either inherent flexibility or to different conformations in the two crystal forms. Region 50–55 shows only few structural constraints in the NMR structure which would support the notion that it might be inherently flexible. In the crystal, RGS-RBD is connected to a symmetry related RBD molecule via disulfide bridges in both crystal forms, although the packing of the molecules is different in each (Fig. 1a, b). Since the crystals took a long time to grow (ca. 6 months), the formation of the correct disulfide bridges might have been the limiting factor for crystallization. The relative orientation of Ras and RGS-RBD is the same in the two crystal forms in spite of the different crystal contacts and packing, indicating that the complex structure is not disturbed by the disulfide bridges. The overall structure of the complex is shown in Fig. 1c as a ribbon plot. Contrary to the results of Huang et al. [2], one Ras molecule interacts with only one RGS-RBD molecule in both of our crystal forms. Therefore we believe dimerization to be caused by crystal packing, consistent with biochemical studies (see below).

The major feature of the interaction is the alignment of the two proteins along the outer strands of their β-sheets such that an apparent continuous β-sheet between the two proteins is formed, similar to what was found for the wild-type Rap·RafRBD complex [1], and for the mutant Raps·RafRBD complex believed to be a good mimic of the Ras·RafRBD complex [18] (Fig. 1c, d), and has also been shown for the mutant Ras·RGS-RBD complex [2]. The dissociation of nucleotide is inhibited by the binding of the RalGDS effector [25] but as in the RafRBD complex, this effect is indirect as the nucleotide-binding site is not directly involved in or situated at the interface of the complex [1,18]. The structure of RGS-RBD is not changed appreciably as the superposition of free RGS-RBD from both the NMR and X-ray determination [28,29] together with complexed protein shows no large deviation and has an rms difference of 2.4 and 1.8 Å for 60 Cα atoms, respectively (not shown).

As mentioned above, RGS-RBD and RafRBD share the same fold and overlay quite well with an rms difference of 3.6 Å for 49 Cα atoms (Fig. 2a). However, if Ras and Rap from the complexes are superimposed, the corresponding RBDs are rotated by approximately 35° when viewed from the direction of the Ras or Rap moiety (Fig. 2b). In the Rap·RafRBD complex, the β-sheet of the RBD nicely continues the β-sheet of Ras, whereas in the Ras·RGS-RBD the two adjacent β-strands of Ras and RGS-RBD are tilted due to the 35° rotation. However, the number of possible main chain interactions which are typical for a β-sheet is about the same in the two complexes and quite small since the majority of the interactions is formed by side chains.

3.2. Structural and biochemical analysis of the interface

As seen with higher resolution for the Ras mutant [2], the interaction between Ras and RGS-RBD is between the first two β-strands and the long helix α1 of the RBD using the mostly hydrophilic side chains of Arg-16, Lys-28, Ser-29 and Lys-48 of RGS-RBD, similar to the interaction between RafRBD and Rap and the Ras homologue Raps [1,18] as shown schematically in Fig. 3. Similar hydrophilic residues of RGS-RBD and RafRBD are involved in the binding of Ras, although it is obvious that RGS-RBD has less positively

Table 1
Data collection

	Crystal 1	Crystal 2
Space group	$C222_1$	$P6_322$
Unit cell	$a = 53.4$ Å	$a = b = 94.3$ Å
	$b = 96.0$ Å	$c = 164.8$ Å
	$c = 105.9$ Å	
Resolution	45–3.4 Å	35–3.4 Å
Unique reflections	8824	4528
Observed reflections	89647	14741
Completeness	99.3%	90.2%
Completeness 3.5–3.4 Å	98.0%	72.1%
$\langle I/\sigma \rangle$	16.3	20.1
$\langle I/\sigma \rangle$3.5–3.4 Å	2.3	7.9
R^a_{sym}	16.0%	9.1%
R^a_{sym} 3.5–3.4 Å	67.4%	14.0%
R_{crys}b	30.9%	
R_{free}	35.4%	
Molecular replacement[c]: R factor	42.3%/50.6%	40.7%/51.6%
Molecular replacement[c]: correlation	44.0/14.6	51.8/15.0

[a] $R_{sym} = \Sigma_{hkl}\Sigma_i\ |I_i - \langle I \rangle| / \Sigma_{hkl}\Sigma_i\ I_i$, where I_i is the intensity for the ith measurement of an equivalent reflection with indices h, k, l.
[b] $R_{crys} = \Sigma_{hkl}||F_{obs}| - |F_{calc}|| / \Sigma_{hkl}|F_{obs}|$, where F_{obs} denotes the observed structure factor amplitude and F_{calc} denotes the structure factor amplitude calculated from the model. 10% of reflections were used to calculate R_{free}.
[c] For both molecular replacements, Ras·GTP was used as model (PDB code 5p21). The values after the slash are the R factors and correlations of the second highest peak.

charged residues in the interface. On the Ras side residues Asp-33, Pro-34, Ile-36, Glu-37, Asp-38, Ser-39 and Tyr-40 from the switch I region are involved in the interaction. Both effectors Raf and RalGDS share common binding partners on Ras, differences are seen for residues Glu-31, Ser-39 and Arg-41 which interact with RafRBD but not with RGS-RBD (Fig. 3), whereas Pro-34 and Tyr-40 interact with RGS-RBD but not with RafRBD.

To relate the structural findings with a more quantitative analysis of the interaction and to determine the importance of individual amino acids, the affinity of the Ras·RGS-RBD complex in solution was investigated with appropriate mutants of RGS-RBD and Ras. The basic residues Arg-16, Lys-28 and Lys-48 on RGS contribute strongly to the interaction, whereas other residues close to the interface such as Asn-23, Asn-25 or Tyr-27 have a weaker effect (Table 2). RGS-RBD contains a stretch of four consecutive glutamic acid residues between α1 and β3, the charge but not the sequence of which is conserved in RalGDSs. They have been found to be involved in binding to a Ras (E31K) mutant in the crystal structure of its complex with RGS-RBD [2]. Mutants E52A and E53A show a slightly stronger binding to wild-type Ras, as if these residues had an inhibitory effect on the interaction.

Glu-37 forms only a weak ionic interaction with Arg-16 of RalGDS. Correspondingly the affinity of Ras(E37G) is reduced only 1.6-fold (Table 2), in line with the assumption from transfection experiments that this mutant is still inducing the RalGDS pathway, whereas Glu-37 is crucial for the Raf pathway [6–12]. From residues mutated in Ras, Thr-35, Asp-38 and Tyr-40 have apparently the strongest effect on binding energy. D38A is a very drastic mutation which seems to effect all Ras pathways, whereas the somewhat weaker D38E allele is still able to interact with Raf kinase [7]. Asp-38 is the most important contact residue in the RGS-RBD complex and is located close to the residues Lys-28 and Lys-48. The D38E mutation might disturb the network of charges around residues Asp-33, Asp-38 of Ras and Lys-28, Lys-48 of RGS-RBD, but not in the RafRBD interface with Lys-28 replaced by Thr-68, explaining its selective biological action. Tyr-40 forms a considerable part of the contact surface, forming numerous hydrophobic and hydrophilic contacts which would explain the loss of affinity of the Y40C mutant.

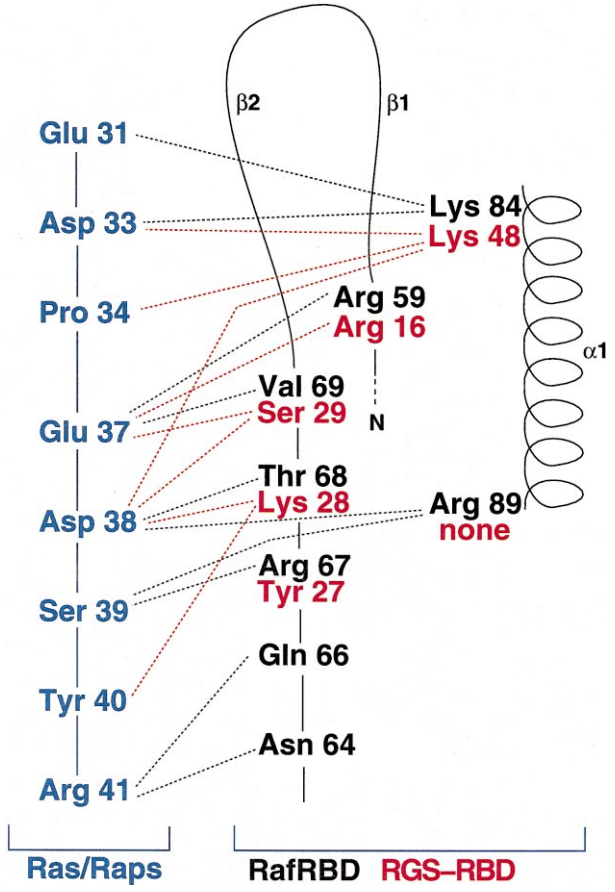

Fig. 3. Schematic comparison of the interactions of Ras with RGS-RBD as compared to those of Raps (Rap mutant with D30E, E31K) with RafRBD [1,18].

It had been anticipated that Thr-35 would be involved in the interface since the mutation T35S reduces the affinity to RGS-RBD at least 30-fold (Table 2). Surprisingly the structure of the Ras·RGS-RBD complex shows no direct involvement of Thr-35 in complex formation. In the structure of the Ras(E31K)·RGS-RBD complex described by Huang et al. [2] an indirect interaction between the hydroxyl side chain of Thr-35 and Lys-52 via a water molecule was shown. However such an interaction should also be possible with a Ser-35 side chain. The reduced affinity for RGS-RBD is thus not obvious from the X-ray structures.

3.3. Ras versus Rap signaling

Both Ras and Rap bind to the same set of effectors in vitro which is not surprising considering the similar effector regions, although in vivo Rap appears to have a different biological function [32]. RafRBD binds Ras about 100-fold tighter than Rap [25], and the difference is due to an unfavorable interaction between Lys-84 of RafRBD and Lys-31 of Rap, which is Glu in Ras [1,18]. The opposite relative affinity is found for RGS-RBD, with high affinity to Rap and about 100-fold lower for Ras, with the mutation of Glu-31 in Ras to lysine increasing the affinity (Table 2; [25]). In the structure of the complex of RGS-RBD with the E31K mutant of Ras [2], Lys-31 was found to interact with the side chains of Asp-51, Asn-54 and Asp-56 (corresponding to Asp-47, Asn-50 and Glu-52 in human RalGDS used here). In the wild-type Ras·RGS-RBD complex this highly charged loop appears disordered and does not show a direct interaction. A possible explanation might be the long-range charge-charge interactions across the interface. The strong negative potential caused by the highly negatively charged loop 52–58 (L3) of RGS-RBD, as seen from the isopotential contours of the RGS-RBD moiety in the Ras·RGS-RBD complex appears to interfere with Glu-31 (not shown). In support of this, the less negatively charged mutants E52A, E53A and E52K of RGS-RBD show a slightly higher affinity to Ras (Table 2). The increase in affinity to RalGDS due to charge reversal at position 31 is highlighted by the X-ray structure of the Ras(E31K) complex, where Lys-31 makes contact to three Asp/Asn residues of the α1-L3 region [2].

Table 2
Mutational data

Ras mutants		
Ras WT·wtRGS-RBD	3.5[a]	K_D ratio, Mut/WT
Ras(E31K)·	0.12	0.034
Ras(T35S)·	>100	29
Ras(E37G)·	5.5	1.6
Ras(D38A)·	100	29
Ras(Y40C)·	100	29
Ras(E63A)	3.1	0.9
RGS-RBD mutants		
RasWT·RGS-RBD WT	3.5[a]	K_D ratio, Mut/WT
·R16A	100	29
·N23A	11.0	3.1
·N25A	5.6	1.6
·Y27F	29.0	8.3
·K28A	100	29
·K48A	100	29
E52A	2.1	0.6
·E53A	2.5	0.7
·E53K	1.8	0.5

Equilibrium dissociation constants (K_D, in μM) of the complex between wild-type and mutated Ras and RGS-RBD, measured as described in Section 2.
[a]The K_D values here are higher compared to [25] since the buffer contained additional 100 mM NaCl.

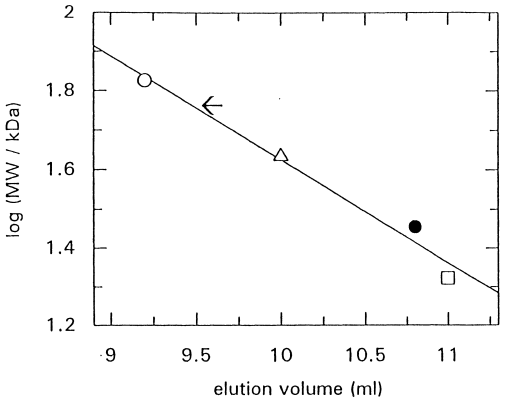

Fig. 4. Size exclusion chromatography (Superdex 75 10/30, Pharmacia) with calibration proteins bovine serum albumin ○ (66 kDa), ovalbumin △ (43 kDa) and H-Ras □ (21 kDa), and with the Ras·RGS-RBD complex ● (29 kDa). The arrow indicates the elution volume expected for a dimeric complex of Ras·RGS-RBD.

3.4. Involvement of switch II and stoichiometry of the Ras·RGS-RBD complex

In the structure presented here, switch II region of Ras is not involved in the interaction. Glu-63 in switch II was found to be involved in a number of contacts with a second molecule of RGS-RBD in the crystal of the Ras(E31K)·RGS-RBD complex [2]. However, Glu-63 can be mutated to Ala without any effect on affinity, strengthening the assumption that the interaction of RGS-RBD with switch II found in the Ras(E31K) mutant structure is not relevant for complex formation in solution. To further address the question if the complex of Ras and RGS-RBD forms a dimer in solution, size exclusion chromatography was applied to the proteins. This technique is based on the linear relationship between the logarithm of the molecular weight (MW) of the proteins and their elution volume. Fig. 4 shows the elution volume for the Ras·RGS-RBD complex, which is found at a position which corresponds to the monomer form. For comparison the calculated elution volume for the dimer complex is indicated by an arrow. This finding supports our notion that the dimer formation via the switch II region observed in the Ras(E31K) mutant structure [2] is due to packing in the crystal and that the interaction between Ras and RGS-RBD does only involve the switch I region of Ras.

References

[1] Nassar, N., Horn, G., Herrmann, C., Scherer, A., McCormick, F. and Wittinghofer, A. (1995) Nature 375, 554–560.
[2] Huang, L., Hofer, F., Martin, G.S. and Kim, S.-H. (1998) Nat. Struct. Biol. 5, 422–426.
[3] McCormick, F. and Wittinghofer, A. (1995) Curr. Opin. Biotechnol. 7, 449–456.
[4] White, M.A., Nicolette, C., Minden, A., Polverino, A., Van Aelst, L., Karin, M. and Wigler, M.H.. (1995) Cell 80, 1–20.
[5] Akasaka, K., Tamada, M., Wang, F., Kariya, K., Shima, F., Kikuchi, A., Yamamoto, M., Shirozu, M., Yokoyama, S. and Kataoka, T. (1996) J. Biol. Chem. 271, 5353–5360.
[6] Rodriguez-Viciana, P., Warne, P.H., Vanhaesebroeck, B., Waterfield, M.D. and Downward, J. (1996) EMBO J. 15, 2442–2451.

[7] Rodriguez-Viciana, P., Warne, P.H., Khwaja, A., Marte, B.M., Pappin, D., Das, P., Waterfield, M.D., Ridley, A. and Downward, J. (1997) Cell 89, 457–467.
[8] Khosravi-Far, R., White, M.A., Westwick, J.K., Solski, P.A., Chrzanowska-Wodnicka, M., Van Aelst, L., Wigler, M.H. and Der, C.J. (1996) Mol. Cell. Biol. 16, 3923–3933.
[9] White, M.A., Vale, T., Camonis, J.H., Schaefer, E. and Wigler, M.H. (1996) J. Biol. Chem. 271, 16439–16442.
[10] Joneson, T., White, M.A., Wigler, M.H. and Bar-Sagi, D. (1996) Science 271, 810–812.
[11] Wolthuis, R.M.F., de Ruiter, N.D., Cool, R.H. and Bos, J.L. (1997) EMBO J. 16, 6748–6761.
[12] Murai, H., Ikeda, M., Kishida, S., Ishida, O., Okazaki-Kishida, M., Matsuura, Y. and Kikuchi, A. (1997) J. Biol. Chem. 272, 10483–10490.
[13] Zhang, X.-F., Settleman, J., Kyriakis, J.M., Takeuchi-Suzuki, E., Elledge, S.J., Marshall, M.S., Bruder, J.T., Rapp, U.R. and Avruch, J. (1993) Nature 364, 308–313.
[14] Warne, P.H., Rodriguez-Viciana, P. and Downward, J. (1993) Nature 364, 352–355.
[15] Vojtek, A.B., Hollenberg, S.M. and Cooper, J.A. (1993) Cell 74, 205–214.
[16] van Aelst, L., Bar, M., Marcus, S., Polverino, A. and Wigler, M. (1993) Proc. Natl. Acad. Sci. USA 90, 6213–6217.
[17] Emerson, S.D., Madison, V.S., Palermo, R.E., Waugh, D.S., Scheffler, J.E., Tsao, K.L., Kiefer, S.E., Liu, S.P. and Fry, D.C. (1995) Biochemistry 34, 6911–6918.
[18] Nassar, N., Horn, G., Herrmann, C., Block, C., Janknecht, R. and Wittinghofer, A. (1996) Nat. Struct. Biol. 3, 723–729.
[19] Albright, C.F., Giddings, B.W., Liu, J., Vito, M. and Weinberg, R.A. (1993) EMBO J. 12, 339–347.
[20] Hofer, F., Fields, S., Schneider, D. and Martin, G.S. (1994) Proc. Natl. Acad. Sci. USA 91, 11089–11093.
[21] Spaargaren, M. and Bischoff, J.R. (1994) Proc. Natl. Acad. Sci. USA 91, 12609–12613.
[22] Kikuchi, A., Demo, S.D., Ye, Z.-H., Chen, Y.-W. and Williams, L.T. (1994) Mol. Cell. Biol. 14, 7483–7491.
[23] Wolthuis, R.M.F., Bauer, B., van 't Veer, L.J., de Vries-Smits, A.M., Cool, R.H., Spaargaren, M., Wittinghofer, A., Burgering, B.M. and Bos, J.L. (1996) Oncogene 13, 353–362.
[24] Peterson, S.N., Trabalzini, L., Brtva, T.R., Fischer, T., Altschuler, D.L., Martelli, P., Lapetina, E.G., Der, C.J. and White 2nd, G.C. (1996) J. Biol. Chem. 271, 29903–29908.
[25] Herrmann, C., Horn, G., Spaargaren, M. and Wittinghofer, A. (1996) J. Biol. Chem. 271, 6794–6800.
[26] Kabsch, W. (1988) J. Appl. Cryst. 21, 916–924.
[27] Collaborative Computational Project No. 4. The CCP4 suite: programs for protein crystallography (1994) Acta Cryst. D 50, 760–763.
[28] Geyer, M., Herrmann, C., Wohlgemuth, S., Wittinghofer, A. and Kalbitzer, H.R. (1997) Nat. Struct. Biol. 4, 694–699.
[29] Huang, L., Weng, X., Hofer, F., Martin, G.S. and Kim, S.-H. (1997) Nat. Struct. Biol. 4, 609–615.
[30] Jones, T.A., Zou, J-Y., Cowan, S.W. and Kjeldgaard, M. (1991) Acta Cryst. A 47, 110–119.
[31] Humphrey, D., Kwiatkowska, J., Henske, E.P., Haines, J.L., Halley, D., van Slegtenhorst, M. and Kwiatkowski, D.J. (1997) Ann. Hum. Genet. 61, 299–305.
[32] Bos, J.L. (1997) EMBO J. 17, 6676–6782.
[33] Kraulis, P.J. (1991) J. Appl. Cryst. 24, 946–950.
[34] Nicholls, A., Sharp, K.A. and Honig, B. (1991) Proteins 11, 281–293.